Heterogeneously-Integrated Self-injection Locked Lasers on Thin Film Lithium Niobate

Mingxiao Li[1], Chao Xiang[1], Jonathan Peters[1], Joel Guo[1], Theodore Morin[1], Shixin Xue[2], Mario Dumont[1], Jeremy Staffa[3], Qiang Lin [2,3], and John E. Bowers[1]

1. Department of electrical and computer engineering, University of California, Santa Barbara, Santa Barbara, CA 93106, USA.
2. Department of electrical and computer engineering, University of Rochester, Rochester, NY 14627, USA.
3. Institute of Optics, University of Rochester, Rochester, NY 14627, USA.

Abstract: We demonstrate a heterogeneously integrated self-injection locked lithium niobate laser via direct bonding. The single mode lasing power is as high as 16 mW with a side mode suppression ratio over 50 dB.

OCIS codes: (140.5960) Semiconductor lasers; (130.3730) Lithium niobate

Photonic integration enables system miniaturization which is crucial in advanced applications. With decades of development, silicon photonics has realized numerous achievements in optical communication, signal processing and sensing systems. Undoubtedly, the integration of semiconductor lasers played a critical role in its development. Primary designs of semiconductor lasers are purely III-V based, with monolithic growth on silicon. Recently, increasing effort is devoted to the heterogeneous integration of III-V to passive material platforms where an external cavity design is adopted. This structure benefits the laser performance by extending the cavity to a passive material with lower loss and enhanced functionality [1–3]. Lithium niobate ($LiNbO_3$, LN), as a well-known material with strong second-order nonlinearity and large transparent window is widely applied to numerous areas, including optical communication, microwave optics and signal processing, which makes it a highly demanded material in novel integrated semiconductor lasers. As a result, researchers have investigated a variety of integration approaches, including hybrid integration, transfer printing, flip-chip bonding and dielectric adhesive layer bonding [4–7]. Here we take one step further along this path and demonstrate a heterogeneously integrated laser with lithium niobate via direct bonding, which enables a maximum single mode lasing power of 16 mW on chip and a side mode

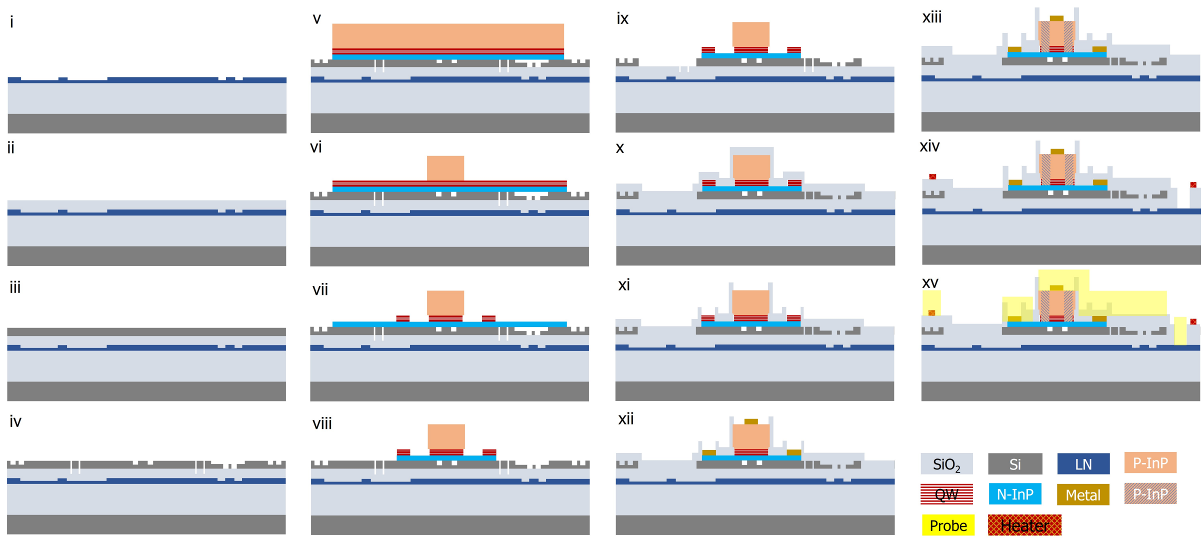

Fig. 1. Multilayer heterogeneous integration process. (i) Lithium niobate wafer patterning. (ii) Silicon dioxide cladding buffer layer deposition and planarization with chemical-mechanical polishing (CMP). (iii) SOI wafer bonding and substrate removal. (iv) Defining gratings and mode transition taper on single crystaline silicon. (v) InP MQW epi pieces bonding. (vi-viii) InP mesa etch. (ix) Excess Si removal. (x-xii) N-/P-metal contact formation. (xiii) Vias open and laser passivation. (xiv) Heaters deposition. (xv) Probe metal formation. All the photolithography steps are performed with a DUV stepper, except for the fine Si grating writing, which uses electron beam lithography. Elements are not shown to scale.

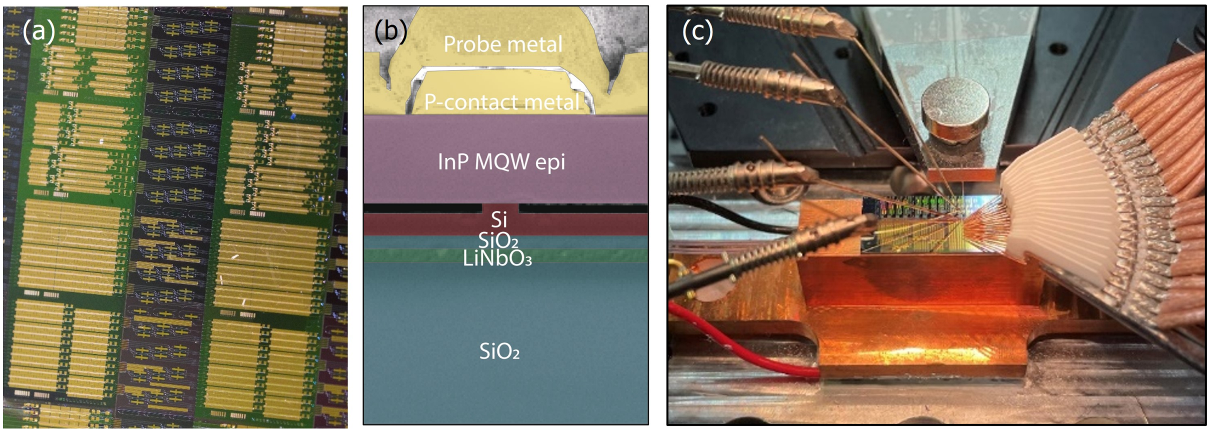

Fig. 2. **(a)** A photo of an array of heterogeneously integrated lasers processed on a 4-inch wafer. Green: bonded single crystalline Si layer. Yellow: gold probe metal and radio-frequency signal electrodes. Dark blue: lithium niobate thin film. **(b)** False-coloured cross section of the multiple quantum well distributed feedback laser with lithium niobate. Image is taken by SEM. **(c)** Measurement setup. A diced chip is placed on a temperature stabilized motion stage; a probe card is adopted for laser current supply; four direct current probes are used for heater and phase shifter control; a motion controlled lensed fiber is employed for output light coupling.

suppression ratio (SMSR) of 50 dB. Moreover, the laser is then self-injection locked (SIL) to a lithium niobate resonator which realized a linewidth reduction of 20 dB.

As shown in Fig. 1, the entire structure includes three different layers, which requires two separate bonding processes. The scanning electron microscopy (SEM) image in Figure 2(b) shows the cross section of our heterogeneous structure. A 4-inch lithium niobate-on-insulator (LNOI) wafer is first patterned with waveguides and resonators. Then a silicon-on-insulator (SOI) stack is directly bonded to the planarized silicon dioxide cladding buffer layer on lithium niobate, followed by a removal of substrate and buried oxide. A Si/LN heterogeneous structure is now formed. After the patterning of DFB gratings and light routing structures on single crystalline silicon, an InP-based multiple quantum well (MQW) epi is then directly bonded to the Si layer, functioning as the gain medium for our distributed feedback laser (DFB) laser. After the laser structure definition, several metal layers are deposited on the wafer for the current supply of lasers and heaters. A passivation step is also performed to form the MQW current channel by hydrogen implantation. Figure 2(a) shows the devices on the 4-inch wafer after the heterogeneous process. The wafer is diced and polished for testing.

We focus on the DFB laser here to demonstrate our device performance. A hybrid InP/Si active waveguide structure is adopted for our laser to realize efficient mode coupling to the Si layer [8]. The laser output is then transferred to the lithium niobate thin film layer with a Si mode transition taper [9]. After that, a lithium niobate resonator is employed to reduce the laser noise via self-injection locking. The output laser power is then measured with a lensed fiber which couples the light from a tapered waveguide at lithium niobate facet.

The experiment setup is shown in Fig. 2(c). A probe card is first adopted for laser current supply. A direct current is then applied to the phase shifter using a set of probes for self-injection locked laser control. While another set of probes apply the current for resonance wavelength tuning to match the lasing wavelength. As shown in Figure 3(a), the laser exhibits a lasing threshold of 150 mA, and a maximum power of 4 mW in fiber at a pumping current of 700 mA, corresponding to 16 mW on chip, accounting for the 6 dB chip to fiber coupling loss. The irregular variation of lasing power along the LI curve shown in Fig. 3(a) is simply due to the mode hoping when the pumping current increases. Additionally, the dip in the LI curve indicates the wavelength matching of laser and resonator. The recorded optical spectrum of the laser is shown in the inset of Fig. 3(a) indicates the single mode lasing at 1559.0 nm with a side-mode suppression ratio (SMSR) of over 50 dB.

The laser linewidth measurement is also performed by recording the frequency noise of the free-running DFB laser. As shown in Figure 3(b), the laser exhibits a white frequency noise floor of 0.33 MHz^2/Hz at the frequency of 40 MHz, corresponding to an intrinsic linewidth of 2.1 MHz. To further improve the performance of our laser, first, we matched our lasing mode to the resonance of the lithium niobate resonator. Then we tuned the phase shifter between the laser and resonator, realizing a self-injection locked laser to reduce the laser linewidth. The noise floor is lowered to 3.5 kHz^2/Hz, corresponding to an intrinsic linewidth of 22.0 kHz, with a noise reduction factor of two orders of magnitude. Current linewidth reduction ratio is limited by the quality factor of the lithium niobate resonator, which could be further improved in the future.

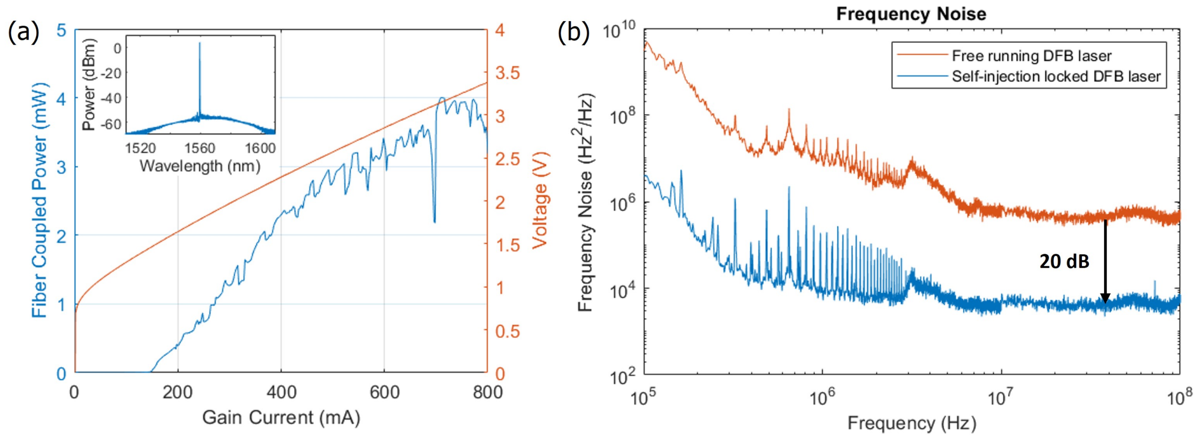

Fig. 3. **(a)** Measured LI curve of the DFB laser on TFLN. The inset shows the single mode lasing spectrum measured by an optical signal analyzer (OSA). **(b)** The calculated frequency noise from the measured phase noise of a free-running DFB laser (orange), and a self-injection locked DFB laser (blue).

In summary, we demonstrated a heterogeneously integrated laser on lithium niobate with a maximum single mode lasing power of 4 mW in fiber and a SMSR of 50 dB, as well as an intrinsic linewidth of 22.0 kHz obtained by self-injection locking. Certainly, more functions could be added to our platform, such as the high-speed electro-optical modulation and intracavity frequency conversion. Consequently, the integration of semiconductor lasers and thin film lithium niobate can not only enable specific applications, including but not limited to the chip-based multi-color lasers, optical transceivers, and LiDAR sources, but also paves the road to fully integrated photonic integrated circuits in optical signal processing systems, nonlinear optics applications, quantum photonics, and optical communications [10–13].

Funded by DARPA LUMOS (HR001-20-2-0044).

References

1. M. A. Tran, D. Huang, and J. E. Bowers, "Tutorial on narrow linewidth tunable semiconductor lasers using Si/III-V heterogeneous integration", *APL Photonics* **4**, 111101 (2019).
2. Y. Fan, A. van Rees, P. J. M. van der Slot, J. Mak, R. M. Oldenbeuving, M. Hoekman, D. Geskus, C. G. H. Roeloffzen, K.-J. Boller, "Hybrid integrated InP-Si3N4 diode laser with a 40-Hz intrinsic linewidth", *Opt. Express* **28**, 21713-21728 (2020).
3. C. Xiang, P. A. Morton, and J. E. Bowers, "Ultra-narrow linewidth laser based on a semiconductor gain chip and extended Si3N4 Bragg grating", *Opt. Lett.* **44**, 3825-3828 (2019).
4. C. O. Beeck, F. M. Mayor, S. Cuyvers, S. Poelman, J. F. Herrmann, O. Atalar, T. P. McKenna, B. Haq, W. Jiang, J. D. Witmer, G. Roelkens, A. H. Safavi-Naeini, R. V. Laer, B. Kuyken, "III/V-on-lithium niobate amplifiers and lasers", *Optica* **8**, 1288-1289 (2021).
5. A. Shams-Ansari, D. Renaud, R. Cheng, L. Shao, L. He, D. Zhu, M. Yu, H. R. Grant, L. Johansson, M. Zhang, and M. Lončar, "Electrically pumped laser transmitter integrated on thin-film lithium niobate", *Optica* **9**, 408-411 (2022).
6. M. Li, L. Chang, L. Wu, J. Staffa, J. Ling, U. A. Javid, S. Xue, Y. He, R. Lopez-rios, T. J. Morin, H. Wang, B. Shen, S. Zeng, L. Zhu, K. J. Vahala, J. E. Bowers, and Q. Lin, "Integrated Pockels laser", *Nature Communications* **13**, 5344 (2022).
7. X. Zhang, X. Liu, L. Liu, Y. Han, H. Tan, L. Liu, Z. Lin, S. Yu, R. Wang, and X. Cai, "Heterogeneous integration of III–V semiconductor lasers on thin-film lithium niobite platform by wafer bonding", *Applied Physics Letters* **122**, 8.(2023).
8. M. L. Davenport, S. Skendžić, N. Volet, J. C. Hulme, M. J. R. Heck and J. E. Bowers, "Heterogeneous Silicon/III–V Semiconductor Optical Amplifiers", *IEEE Journal of Selected Topics in Quantum Electronics*, **22**, 6, (2016).
9. C. Xiang, J. Guo, W. Jin, L. Wu, J. Peters, W. Xie, L. Chang, B. Shen, H. Wang, Q. Yang, D. Kinghorn, M. Paniccia, K. J. Vahala, P. A. Morton, and J. E. Bowers, "High-performance lasers for fully integrated silicon nitride photonics", *Nat Commun* **12**, 6650 (2021).
10. J. Ling, J. Staffa, H. Wang, B. Shen, L. Chang, U. A. Javid, L. Wu, Z. Yuan, R. Lopez-Rios, M. Li, Y. He, B. Li, J. E. Bowers, K. J. Vahala, and Q. Lin, "Self-Injection Locked Frequency Conversion Laser", *Laser and Photonics Reviews*, **2200663** (2023).
11. J. Riemensberger, A. Lukashchuk, M. Karpov, W. Weng, E. Lucas, J. Liu, and T.J. Kippenberg, "Massively parallel coherent laser ranging using a soliton microcomb", *Nature* **581**, 164-170 (2020).
12. D. Zhu, L. Shao, M. Yu, R. Cheng, B. Desiatov, C. J. Xin, Y. Hu, J. Holzgrafe, S. Ghosh, A. Shams-Ansari, E. Puma, N. Sinclair, C. Reimer, M. Zhang, and M. Lončar, "Integrated photonics on thin-film lithium niobate", *Adv. Opt. Photon.* **13**, 242-352 (2021).
13. A. Boes, L. Chang , C. Langrock, M. Yu, M. Zhang, Q. Lin, M. Lončar, M. Fejer, J. Bowers, and A. Mitchell, "Lithium niobate photonics: Unlocking the electromagnetic spectrum", *Science* **379**, 6627 (2023).